Ecological Indicators 70 (2016) 276–284

Contents lists available at ScienceDirect

Ecological Indicators

journal homepage: www.elsevier.com/locate/ecolind

Comparative regional-scale soil salinity assessment with near-ground apparent electrical conductivity and remote sensing canopy reflectance

Elia Scudiero*, Todd H. Skaggs, Dennis L. Corwin

USDA-ARS, United States Salinity Laboratory, 450 West Big Springs Rd., Riverside, CA 92507-4617, USA

ARTICLE INFO

Article history:
Received 10 February 2016
Received in revised form 23 May 2016
Accepted 12 June 2016

Keywords:
Soil salinity mapping
Apparent soil electrical conductivity
Spatial variability
Remote sensing
ANOCOVA

ABSTRACT

Soil salinity is recognized worldwide as a major threat to agriculture, particularly in arid and semi-arid regions. Producers and decision makers need updated and accurate maps of salinity in agronomically and environmentally relevant ranges (i.e., <20 dS m^{-1}, when salinity is measured as electrical conductivity of the saturation extract, EC_e). State-of-the-art approaches for creating accurate EC_e maps beyond field scale (i.e., 1 km^2) include: (i) Analysis Of Covariance (ANOCOVA) of near-ground measurements of apparent soil electrical conductivity (EC_a) and (ii) regression modeling of multi-year remote sensing canopy reflectance and other co-variates (e.g., crop type, annual rainfall). This study presents a comparison of the two approaches to establish their viability and utility. The approaches were tested using 22 fields (total 542 ha) located in California's western San Joaquin Valley. In 2013 EC_a-directed soil sampling resulted in the collection of 267 soil samples across the 22 fields, which were analyzed for EC_e, ranging from 0 to 38.6 dS m^{-1}. The ANOCOVA EC_a-EC_e model returned a coefficient of determination (R^2) of 0.87 and root mean square prediction error (RMSPE) of 3.05 dS m^{-1}. For the remote sensing approach seven years (2007–2013) of Landsat 7 reflectance were considered. The remote sensing salinity model had R^2 = 0.73 and RMSPE = 3.63 dS m^{-1}. The robustness of the models was tested with a leave-one-field-out (*lofo*) cross-validation to assure maximum independence between training and validation datasets. For the ANOCOVA model, *lofo* cross-validation provided a range of scenarios in terms of RMSPE. The worst, median, and best fit scenarios provided global cross-validation R^2 of 0.52, 0.80, and 0.81, respectively. The *lofo* cross-validation for the remote sensing approach returned a R^2 of 0.65. The ANOCOVA approach performs particularly well at EC_e values <10 dS m^{-1}, but requires extensive field work. Field work is reduced considerably with the remote sensing approach, but due to the larger errors at low EC_e values, the methodology is less suitable for crop selection, and other practices that require accurate knowledge of salinity variation within a field, making it more useful for assessing trends in salinity across a regional scale. The two models proved to be viable solutions at large spatial scales, with the ANOCOVA approach more appropriate for multiple-field to landscape scales (1–10 km^2) and the remote sensing approach best for landscape to regional scales (>10 km^2).

Published by Elsevier Ltd.

1. Introduction

Soil salinization diminishes the productivity of irrigated farmlands throughout the world (Ghassemi et al., 1995; Ivits et al., 2011; Singh, 2015). Of the cultivated lands worldwide, about 0.34×10^9 ha (23%) are estimated to be saline and another 0.56×10^9 ha (37%) are estimated to be sodic (Tanji and Wallender, 2012). In actuality, these estimates are educated guesses at best as no reliable quantitative inventories of soil salinity exist due to the dynamic and complex spatial and temporal nature of salinity, which make measurements at regional scale problematic.

Abbreviations: ANOCOVA, Analysis Of Covariance; CRSI, canopy response salinity index; EC_a, apparent soil electrical conductivity (dS m^{-1}); EC_e, electrical conductivity of the saturation extract (dS m^{-1}); EC_aH, apparent soil electrical conductivity measurement taken in the horizontal coil configuration with an electromagnetic induction conductivity meter; EC_aV, apparent soil electrical conductivity measurement taken in the vertical coil configuration with an electromagnetic induction conductivity meter; FSR, field specific regression; OLS, ordinary least square; MAE, mean absolute error; NRCS, natural resource conservation service; RMSPE, root mean square prediction error; WSJV, western San Joaquin Valley.

* Corresponding author.
E-mail addresses: elia.scudiero@ars.usda.gov, scudiero@dmsa.unipd.it (E. Scudiero).

http://dx.doi.org/10.1016/j.ecolind.2016.06.015
1470-160X/Published by Elsevier Ltd.

The U.S. Salinity Laboratory (U.S. Salinity Laboratory Staff, 1954) classifies agricultural soil salinities as: 0–2 dS m^{-1} (non-saline), 2–4 dS m^{-1} (slightly saline), 4–8 dS m^{-1} (moderately saline), 8–16 dS m^{-1} (strongly saline), and >16 dS m^{-1} (extremely saline), where salinity is quantified as the electrical conductivity of a saturated soil paste extract (EC_e, dS m^{-1}). In the agronomically and environmentally relevant ranges of soil salinity (i.e., <20–30 dS m^{-1}), the available regional-scale maps are often qualitative or unreliable (Lal et al., 2004; Lobell, 2010), and, therefore, provide little useful information for producers, land and water resource managers, extension specialists, or policy and decision makers. Methods of quantitatively mapping and monitoring soil salinity at regional to global scales are essential for providing information to land and water resource managers and decision makers faced with policy decisions responding to climate pattern changes and increased food demands that require alternative water sources (e.g., reuse of degraded water) and marginally productive land (e.g., saline-sodic soils).

Two approaches have been presented in the literature as reliable methods to map root-zone soil salinity over large spatial extents (i.e., >1 km^2): (i) the Analysis Of Covariance (ANOCOVA) technique and (ii) multi-year remote sensing techniques. The ANOCOVA technique (Corwin and Lesch, 2014) uses field measurements of apparent soil electrical conductivity (EC_a) as a proxy for soil salinity. Intensive geospatial measurements of EC_a can be acquired over an entire field quickly (e.g., thousands of measurements per day). According to the ANOCOVA technique the EC_a-salinity relationship can be represented with linear modeling. Once this relationship is calibrated over a sufficiently large set of fields, the ANOCOVA approach assumes that the slope coefficients of the EC_a-salinity relationship remain constant throughout the same region, whereas the intercept may vary from field-to-field because of different soil types and agronomic practices. The ANOCOVA technique maps soil salinity based on the EC_a survey data and a single soil sample taken from each field, which is needed to calculate the regression intercept. Alternatively, multi-year remote sensing of canopy reflectance can be used to map salinity at regional scale (Lobell et al., 2010). Freely available satellite data (e.g., Landsat reflectance provided by the U.S. Geological Survey Agency) can be used to model soil salinity with total coverage over the area of interest (e.g., Wu et al., 2014; Yahiaoui et al., 2015). A regression model relates soil salinity to multi-year remote sensing canopy reflectance, usually in the form of a ratio of wavelengths representing a salinity index, and other co-variates (e.g., fallow or cropped, crop type, annual rainfall).

The preferred method for mapping soil salinity at large (multiple-field to regional) scales likely depends on the intended audience and use of the salinity map, and on available resources. The objective of this study is to compare the two available methodologies with respect to accuracy, potential map uses, and required resources. The comparison, which highlights the strengths and weaknesses of the two approaches, will assist decision makers in determining which approach best meets their needs and matches their resources. It also provides scientists with direction for future research efforts that will fill knowledge gaps and improve the quality and efficiency of root-zone salinity mapping at large spatial extents.

2. Theoretical background

2.1. Apparent electrical conductivity estimations of soil salinity with Analysis Of Covariance (ANOCOVA)

Geospatial measurement of apparent (or bulk) soil electrical conductivity (EC_a) is a proximal sensor technique that plays a major role in salinity mapping at field scale (Corwin and Lesch, 2005a). An increase in the concentrations of ions (e.g., Cl^-, Na^+) in the soil solution increases EC_a. Other soil properties also influence EC_a, including texture, water content, bulk density, organic matter, and cation exchange capacity (Corwin and Lesch, 2005a). The EC_a measurements can be expressed as a multiplicative function of salinity, water content, and soil tortuosity (which depends on soil texture, particle pore distribution, density and particle geometry, and organic matter content). Several authors explored this relationship (e.g., Archie (1942) and Rhoades et al. (1976)), which can be generalized as

$$EC_e = \beta \times EM^{\alpha} \times \varepsilon^* \quad (1)$$

where α and β are coefficients that take into account the effects of soil tortuosity and water content; and ε^* is a (multiplicative) error component. In Eq. (1), the error component is the ratio between EC_e and the explanatory term of the equation (Tian et al., 2013).

After a logarithmic transformation of Eq. (1), the EC_a-EC_e relationship is:

$$\ln(EC_e) = \ln(\beta) + \alpha \times \ln(EC_a) + \varepsilon \quad (2)$$

where ε is a random (additive) error component, equal to $\ln(\varepsilon^*)$. Equation [2] can be parameterized using an ordinary least square approach (OLS), provided the underlying assumptions (e.g., residuals are normally distributed and spatially independent) are respected (Lesch and Corwin, 2008). Note that Eq. (2) is not applicable when soil is too dry because the water pathways for electrical conductivity are not continuous. As a rule of thumb, Corwin and Lesch (2013) suggest that volumetric water content should be at least 70% of field capacity when the EC_a survey is carried out.

Field-wide (e.g., 1–100 ha) soil salinity can be mapped using intense geospatial measurements (thousands to tens of thousands per field) calibrated with a limited number of soil sample locations (~6 to 100 per field) using field specific regressions (FSR) of Eq. (2) (Corwin and Lesch, 2005a):

$$\ln(EC_{e,ij}) = \gamma_{0,j} + \gamma_{1,j} \times \ln(EC_{a,ij}) + \varepsilon_{ij} \quad (3)$$

where γ_0 and γ_1 are the OLS regression coefficients and i refers to the location (i.e., latitude and longitude) of the soil samples used to parameterize the model for the field (j) under consideration. Eq. (3) can be used to map specific soil intervals (e.g., 0.6–0.9 m) and/or composite soil profiles (e.g., 0–1.2m). Using the FSR approach to map soil salinity at large spatial extents (i.e., >100 ha) may be unfeasible because the cost of collecting the number of soil samples needed to calibrate Eq. (3) over a large number of fields is prohibitive based on field-work labor and laboratory expenses.

Fortunately, as shown by Corwin and Lesch (2014), when EC_a is measured with volumetric water content at or near field capacity, the γ_1 coefficient can be considered constant across fields in the same region, whereas γ_0 changes from field to field because of differences in soil properties and agricultural management. Therefore, Corwin and Lesch (2014) formulated the ANOCOVA model to calibrate the EC_a-EC_e relationship:

$$\ln(EC_{e,ij}) = \gamma_{0,j} + \gamma_1 \times \ln(EC_{a,ij}) + \varepsilon_{ij} \quad (4)$$

in which the intercept parameter is uniquely estimated for each field, but the slope coefficient is assumed to be constant for a particular geographical region. Once Eq. (4) is parameterized over a number of calibration fields, then salinity can be mapped at a new field using an intense survey of EC_a and a single soil sample EC_e measurement (used to calculate γ_0 for a given field j). The ANOCOVA approach is a significant advance in comparison to the FSR approach in terms of soil sampling labor and laboratory analysis cost.

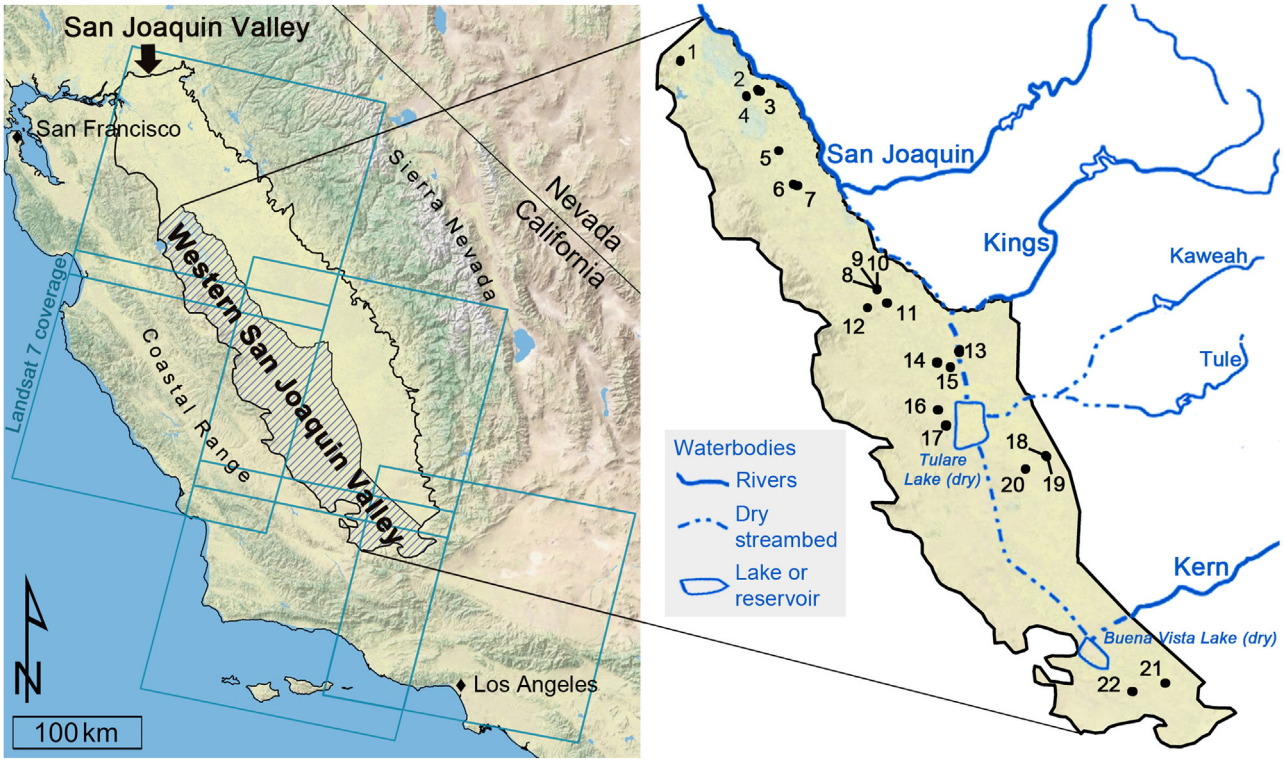

Fig. 1. Map of California's San Joaquin Valley. The western San Joaquin Valley (WSJV) is highlighted with hatch marks. The squares represent the five Landsat 7 tiles covering the WSJV. The location of the 22 study sites is shown in the detailed WSJV map (right). Fields 8, 9, and 10 and fields 18 and 19 are contiguous. Figure is modified from Scudiero et al. (2014).

2.2. Remote sensing of soil salinity

A less expensive means of mapping soil salinity in terms of required field work and laboratory analyses is possible with multi-temporal remote sensing data of canopy reflectance combined with data on environmental covariates such as meteorological data and crop cover information (Lobell et al., 2010; Scudiero et al., 2015; Zhang et al., 2015). When plants experience biotic and abiotic stress (including salinity), their photosynthetic activity decreases, causing increased visible reflectance and reduced near-infrared reflectance (NIR) from the vegetation (Mulla, 2013). Multi-year canopy reflectance data can be used to discriminate landscape features/stressors (e.g., soil salinity), which are relatively stable in time from other, more transient stress types (e.g., drought, pests, and mismanagement). This approach was first developed by Lobell et al. (2010), who used 6 years of MODIS (NASA) reflectance data (250×250 m spatial resolution) to map salinity in the 0–20 dS m^{-1} range in the Red River Valley of eastern North and South Dakota and western Minnesota, USA. Recently, Scudiero et al. (2015) tested this approach using Landsat 7 ETM+ (NASA and USGS) reflectance data (30×30 m spatial resolution) to map salinity in the 0–35 dS m^{-1} range in California's San Joaquin Valley, USScudiero et al. (2015) modeled salinity as:

$$EC_{e,i} = \delta_0 + \delta_{crop} \times CRSI_i + \delta_1 \times RAIN_i + \delta_2 \times TEMP_i + \varepsilon_i \quad (5)$$

where CRSI is the multi-year maximum value (at each 30×30 m location i) of the crop response salinity index (Scudiero et al., 2014); RAIN (mm) is the annual rainfall (from the year with maximum CRSI); TEMP (°C) is the annual average minimum temperature (from the year with maximum CRSI); and δ_0, δ_{crop}, δ_1, and δ_2 are the regression parameters. The δ_{crop} coefficient has two values, one for cropped (i.e., any herbaceous crop and pasture land) and one for fallow (e.g., covered with halophyte weeds) soils. The CRSI is calculated from the blue (B, 450–520 nm), green (G, 520–600 nm), red (R, 630–690 nm), and near-infrared (NIR, 770–900 nm) bands of the ETM+ sensor:

$$CRSI = \sqrt{\frac{(NIR \times R) - (G \times B)}{(NIR \times R) + (G \times B)}} \quad (6)$$

3. Materials and methods

3.1. Apparent electrical conductivity and soil salinity measurements

This study uses the western San Joaquin Valley (WSJV) (Fig. 1) salinity ground-truth measurements originally presented by Scudiero et al. (2014), where a description of the experimental details can be found. The WSJV is one of the most economically important agricultural regions in the USA (Cone, 1997), and has a well-known history of salinity management issues (Chang and Silva, 2014). Soil salinity in the WSJV is affected by numerous geological, meteorological, and management factors. The WSJV's soils are derived from Coastal Range alluvium that was high in salt content due to its geologic origins (Letey, 2000). Salinity naturally accumulates in the surface soils of the semi-arid WSJV because precipitation is not sufficient to leach salts from the root zone. Historically, salinity accumulated along the valley trough (e.g., in the proximity of the San Joaquin and Kings Rivers) (Harradine, 1950), where the ground water table is generally shallow (e.g., 2 m). Long-term irrigation with non-saline water starting in the 1940s reduced the extent of saline soils in WSJV (Schoups et al., 2005).

Throughout 2013, the WSJV was surveyed for soil salinity (Scudiero et al., 2014). Fields (i.e., a continuous section of land farmed with consistent crop and agronomic practice) were selected to represent the full range and frequency distribution of expected soil salinity in the WSJV. SSURGO data were used to identify areas of interest with different salinity levels, and candidate fields were

selected across the WSJV. Finally, land owners were contacted, and field access was granted to 22 fields. Intensive electromagnetic inductions surveys were conducted at the 22 sites (total area 542 ha) collecting 41779 apparent electrical conductivity (EC_a) readings (150–13400 measurements per field, at an average density of 175 per ha^{-1}), for both the 0–0.75 (EC_aH) and 0–1.50 (EC_aV) m soil profiles using an EM38 Dual Dipole (Geonics Ltd., Mississauga, Ontario, Canada) sensor, connected to a GPS, and mounted on a non-metallic sled. The surveys followed the EC_a-directed sampling protocols of Corwin and Lesch (2013) and Corwin and Lesch (2005b). The EC_a readings were analyzed using the ESAP software package (Lesch, 2005; Lesch et al., 2000). A soil sampling scheme was established based on local variations in EC_a across a field using the Response Surface Sampling Design algorithm in ESAP (Lesch, 2005). Soil was sampled at 267 locations over the 22 fields (6–50 sites per field, average density of 0.42 sample ha^{-1}) at 0–0.3, 0.3–0.6, 0.6–0.9, 0.9–1.2, and 1.2–1.5 m. At each of the 267 soil sampling locations, salinity (i.e., electrical conductivity of the soil saturation extract, EC_e, dS m^{-1}) and saturation (SP) were measured (Rhoades, 1996).

3.2. Remote sensing and environmental covariates

This study considers seven years (2007–2013) of Landsat 7 ETM+ (NASA and USGS, USA) canopy reflectance, over five L7 tiles (Fig. 1), covering the entire WSJV, as described by Scudiero et al. (2014). A total number of 366 scenes with cloud coverage <10% were considered. All scenes were corrected through the Landsat Ecosystem Disturbance Adaptive Processing System (LEDAPS) according to Masek et al. (2006). The missing data due to the failure of the Scan Line Corrector were masked according to Roy et al. (2010). On a yearly basis, the L7 scenes were stacked and averaged, producing seven datasets for each of the six multispectral bands. Yearly average values of the Canopy Response Salinity Index (CRSI) were calculated. From the yearly average CRSI, the multi-year maximum CRSI was calculated at each pixel, similarly to that proposed by Wu et al. (2014). The multi-year maxima approach helps isolate the effects of soil salinity from other, less-stable factors (Lobell et al., 2010). Even though this manuscript considers CRSI for the salinity assessment models, similar results (but with weaker goodness-of-fit), and equivalent conclusions, can be achieved with other vegetation indices (Scudiero et al., 2014), such as the normalized difference vegetation index, NDVI (Rouse et al., 1973) and the Enhanced Vegetation Index, EVI (Huete et al., 2002). As discussed by Scudiero et al. (2015), over different geographical regions, the relative performance of different vegetation indices could be different.

Meteorological data (annual rainfall and average minimum temperature) for the remote sensing salinity assessment model in Eq. (5) were obtained from the Parameter-elevation Relationships on Independent Slopes Model (PRISM) (Daly et al., 2008). PRISM provides monthly meteorological data on a 4×4 km cell support. Information on crop cover type were obtained (on a 30×30 m support) from the CropScape database (Han et al., 2012), which presents an easily accessible version of the Cropland Data Layer (Boryan et al., 2011).

Scudiero et al. (2015) developed Eq. (5) using FSR estimations of EC_e, which were interpolated (kriging) on a 30×30 m support, resulting in ca. 6000 ground-truth pixels. Only the ground-truth salinity values from the 267 soil sampling locations are considered herein to compare the remote sensing and ANOCOVA approaches over the same dataset. Two types of ground-truth will be used at the 267 locations: (i) with the assumption of homogeneity within a single EMT+ pixel, a point-support ground-truth dataset will be considered, using the value from the soil analyses at each location and (ii) allowing for heterogeneous pixels, the FSR-interpolated values over the 267 pixels including the soil sampling locations will be used as block-support ground-truth.

Scudiero et al. (2015) approximated the root-zone depth as 1.2 m. In this paper, the remote sensing salinity estimations use the same depth interval. For direct comparison, the ANOCOVA model is also developed for the same soil depth.

3.3. Quality assessment

In spatial datasets, neighboring records tend to be very similar, therefore, traditional cross-validation (CV) methods can lead to almost identical data values in the training and the validation datasets, returning biased predictions (Ruß and Brenning, 2010) with overly optimistic low errors (Brenning, 2012; Ruß and Brenning, 2010). In order to assure spatial independence between training and validation datasets, the salinity assessment models were (cross-) validated through leave-one-field-out (*lofo*) re-sampling, as described in the following paragraphs.

For the ANOCOVA, the common slope (γ_1) coefficient and the field-specific intercept (γ_0) coefficients were estimated over 21 fields (training dataset). The γ_1 coefficient was then used at the validation field to estimate γ_0 at every soil sample location. This was repeated, in turn, for each of the 22 fields. This resulted in multiple ANOCOVA prediction series at each field (i.e., as many as the number of soil samples), which were evaluated using the root mean square prediction error (RMSPE), on the back-transformed data, as follows:

$$\mathrm{RMSPE} = \sqrt{\frac{1}{N_{ij}} \times \sum_{i,j} \left(y_{ij} - \hat{y}_{ij,(-ij)}\right)^2} \tag{7}$$

where $y_{ij} = EC_{e,ij}$ and $\hat{y}_{ij,(-ij)}$ represents the EC_e prediction at the left-out field for the i^{th} locations not used to calculate γ_0. Consequently, each left-out field was characterized by several ANOCOVA prediction scenarios from the i^{th} locations: the best (lowest RMSPE), median (median RMSPE), and worst (highest RMSPE) fits from the i^{th} locations for each field will be discussed.

For the remote sensing modeling, the *lofo* was similar to a classical *k-fold* cross-validation in which each field represented a fold. The *lofo* predictions for the remote sensing approach were evaluated using the RMSPE between observed EC_e values and predictions at the left-out field. Details on this kind of cross-validation and comparison with the traditional (non-spatial) *k-fold* counterpart can be found in Scudiero et al. (2015).

Comparisons were carried out on the validation predictions globally, and within the 0–2 (non-saline), 2–4 (slightly saline), 4–8 (moderately saline), 8–16 (strongly saline), and >16 (extremely saline) dS m^{-1} salinity intervals. The goodness-of-fit of the ANOCOVA and remote sensing salinity predictions were also compared to the FSR salinity estimations. As previously discussed, the FSR salinity estimations are the best field-scale estimations of soil salinity, and are used as ground-truth values in this manuscript. The OLS calibrations and validations of Eq. (4) and Eq. (5) were carried out by Generalized Reduced Gradient nonlinear optimization (Lasdon et al., 1978) using Solver (Frontline Systems, Incline Village, NV, USA) in Microsoft Office Excel 2007 (Redmond, WA, USA).

4. Results

4.1. FSR and ANOCOVA salinity predictions

The 0–1.2 m EC_e at the 267 sampling locations had mean, minimum, maximum, and standard deviation values of 11.6, 0.4, 38.6, and 8.1 dS m^{-1}, respectively. Preliminary correlation analyses indicated that the EC_a measurements for 0–0.75 m could be disregarded from the FSR and ANOCOVA models and the FSR and ANOCOVA

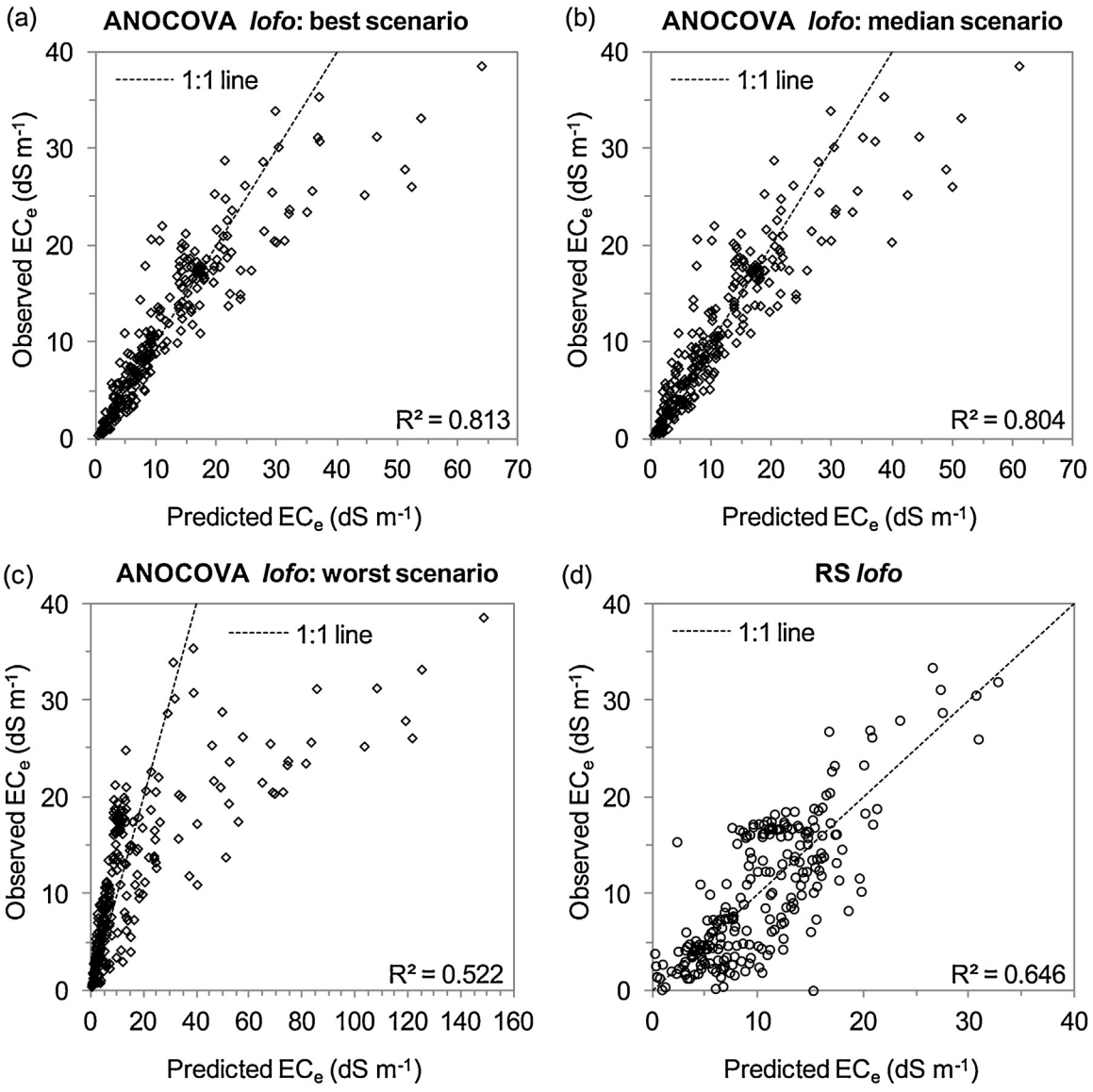

Fig. 2. Leave-one-field-out (*lofo*) cross-validation for the Analysis Of Covariance (ANOCOVA) salinity (ECe) estimations: (a) best-, (b) median-, and (c) worst- fit scenarios. (d) The *lofo* cross-validation for the remote sensing (RS) salinity estimation model. The 1:1 line relationship is reported with a dashed line. Please note the difference scales of the abscissas axes (i.e., predicted values) between quadrants.

models were best established using EC_a readings over the 0–1.5 m depth (i.e., EC_aV). The results for EC_aV were 2.1, 0.1, 6.8, and 1.1 dS m^{-1}, respectively. EC_e and EC_aV had a Pearson's correlation coefficient of 0.85.

The field specific regression (FSR) model (Eq. (3)) was characterized by a coefficient of determination (R^2) of 0.95. When the data was back-transformed, the observed-estimated relationship had $R^2 = 0.93$ and mean absolute error (MAE) = 1.49 dS m^{-1}. In particular, MAE was 0.35, 0.77, 1.07, 1.58, and 2.30 dS m^{-1} for the non-saline, slightly saline, moderately saline, strongly saline, and extremely saline EC_e intervals.

The ANOCOVA model (Eq. (4)) had a slightly lower R^2 (0.92). The back-transformed observed-estimated relationship had $R^2 = 0.88$ and MAE = 2.00 dS m^{-1}. For the non-saline, slightly saline, moderately saline, strongly saline, and extremely saline EC_e intervals, the MAE were 0.46, 0.92, 1.12, 1.98, 3.46 dS m^{-1}, respectively. Table 1 reports the field-specific intercept ($\gamma_{0,j}$) coefficient values and standard errors for Eq. (4). All coefficients were characterized by very small standard errors. As expected, the field-specific $\gamma_{0,j}$ varied remarkably across the valley, with minimum $\gamma_0 = 0.69$ at Field 10 and maximum $\gamma_0 = 2.08$ at Field 17. The common slope (γ_1) was 0.99 (standard error = 0.05).

Across the 22 *lofo* cross-validation iterations, γ_1 was on average 1.01 with a standard deviation of 0.07. The field-specific $\gamma_{0,j}$ coefficients (i.e., intercept) were on average very close to those shown in Table 1, with standard deviations (across the 22 *lofo* iterations) never bigger than 5.7% of the coefficient value. The estimations of γ_1 in the training dataset were used to calculate the γ_0 at each soil sampling location of the left-out field. Table 2 reports the average and standard deviation validation values for γ_0 at the 22 fields. The differences between the $\gamma_{0,j}$ in Table 1 and the average $\gamma_{0,j}$ values obtained in the validation process were minimal (with the exception of Fields 15 and 16). The variability in the calculated validation γ_0 throughout different soil sampling locations for all fields was fairly small, as shown by the low standard deviations in Table 2.

When back-transformed, the best-, median-, and worst-fit *lofo* validations were characterized by R^2 of 0.81 (Fig. 2.a), 0.80 (Fig. 2.b), and 0.52 (Fig. 2.c) and RMSPE of 4.50, 4.55, and 18.58 dS m^{-1}, respectively. In particular, the best validation RMSPE in the different salinity classes were 0.56, 1.20, 1.50, 2.96, and 7.57 dS m^{-1},

Table 1
Analysis Of Covariance (ANOCOVA) field (j) specific intercepts (γ_0) at the 22 fields (F).

Field	F1	F2	F3	F4	F5	F6	F7	F8	F9	F10	F11
$\gamma_{0,j}$	1.56	1.05	0.85	1.35	1.74	0.69	1.11	1.33	1.21	1.17	1.27
Std. err.	0.1	0.11	0.1	0.12	0.14	0.11	0.11	0.06	0.07	0.09	0.11
Field	F12	F13	F14	F15	F16	F17	F18	F19	F20	F21	F22
$\gamma_{0,j}$	1.98	1.08	0.93	1.95	1.96	1.89	0.82	1.38	1.72	2.08	1.56
Std. err.	0.06	0.11	0.08	0.07	0.11	0.09	0.11	0.11	0.11	0.11	0.11

Table 2
Average Analysis Of Covariance (ANOCOVA) field-specific intercepts ($\gamma_{0,j}$) calculated at each of the 22 fields (F) in the leave-one-field-out validation procedure.

Field	F1	F2	F3	F4	F5	F6	F7	F8	F9	F10	F11
Number of samples	8	6	7	6	6	6	6	25	24	10	6
$\gamma_{0,j}$	1.56	1.05	0.84	1.33	1.74	0.68	1.12	1.34	1.22	1.06	1.27
Std. dev.	0.28	0.29	0.46	0.39	0.1	0.51	0.42	0.19	0.22	0.15	0.32
Field	F12	F13	F14	F15	F16	F17	F18	F19	F20	F21	F22
Number of samples	50	6	12	40	6	12	6	6	6	6	6
$\gamma_{0,j}$	1.95	1.08	0.94	1.74	1.84	1.89	0.82	1.31	1.72	2.08	1.56
Std. dev.	0.18	0.29	0.41	0.36	0.28	0.2	0.36	0.48	0.47	0.2	0.19

respectively, for the non-saline, slightly saline, moderately saline, strongly saline, and extremely saline EC_e intervals; for the median fit the RMSPE were 0.67, 1.30, 2.06, 3.20, and 7.27 dS m^{-1}, respectively; and for the worst-fit validation RMSPE were 0.99, 2.81, 3.66, 8.32, and 32.34 dS m^{-1}, respectively.

4.2. Remote sensing salinity predictions

As described in the Materials and Methods section, ground-truth for the remote sensing model (Eq. (5)) was available as point-support (the actual soil analyses were used to represent the entire 30 × 30 m Landsat pixel) and block-support (the FSR EC_e estimations were interpolated over a 30 × 30 m block support). The frequency statistics for the block-support salinity dataset had mean, minimum, maximum, and standard deviation values of 9.87, 0.01, 33.39, 7.03 dS m^{-1}, respectively. These values were fairly similar to those of the point-support dataset (see section 4.1).The calibration of Eq. (5) over the point-support ground-truth dataset returned a R^2 = 0.65 and MAE = 3.52 dS m^{-1}. Better goodness-of-fit was achieved by using the block-support ground-truth dataset: the parameterization of Eq. (5) had R^2 = 0.74 and MAE = 2.79 dS m^{-1}. The remote sensing model is shown in Eq. (8) with the coefficient standard errors reported in parenthesis:

$$EC_{e,i} = 68.7\,(\pm 9.6) + \delta_{crop} \times CRSI_i + 0.018\,(\pm 0.003) \times RAIN_i + 3.02\,(\pm 0.45) \times TEMP_i + \varepsilon_i \quad (8)$$

where δ_{crop} is −141.1 (±5.7) and −138.8 (±6.1) for cropped (i.e., any herbaceous crop) and fallow (e.g., covered with halophyte weeds) soils, respectively. This model was selected for comparison with the ANOCOVA approach.

The validation of the block-support remote sensing model (Fig. 2.d) was characterized by an observed-predicted relationship with R^2 = 0.65 and RMSPE = 4.16 dS m^{-1}. For the non-saline, slightly saline, moderately saline, strongly saline, and extremely saline intervals the RMSPE were 4.54, 3.70, 2.99, 4.42, and 4.99 dS m^{-1}, respectively.

5. Discussion

It is interesting that the FSR EC_a-EC_e calibration (R^2 = 0.93) was only slightly better than that of the ANOCOVA EC_a-EC_e calibration (R^2 = 0.88). This result underlines the robustness of the ANOCOVA approach as a means to reduce the number of soil samples needed to map soil salinity using EC_a measurements. The ANOCOVA *lofo* validations returned very high goodness-of-fit scores. The relatively poor performance of the worst case scenario (Fig. 2.c) is primarily due to Field 15. If Field 15 is removed, then the RMSPE drops from 18.6 to 4.7 dS m^{-1}.

In previous studies (Corwin and Lesch, 2014; Harvey and Morgan, 2009) the ANOCOVA approach was applied to much smaller areas than the WSJV. The values of the FSR γ_1 coefficients were studied to evaluate whether the WSJV should be considered a single ANOCOVA region or if it is too big for such a designation. The FSR γ_1 is not correlated with easting and northing coordinates and according to Moran's spatial autocorrelations statistics (Cliff and Ord, 1981), its values are randomly distributed across the WSJV. According to the US Natural Resources Conservation Service (NRCS) Soil Survey Geographic database (SSURGO), different soil Orders are present in the WSJV (see Scudiero et al., 2014). Yet, there is no evident influence of the different soil Orders on the field specific γ_1 in the FSR approach. This confirms that the ANOCOVA approach can be applied over a regional scale. Future studies should focus on testing the ANOCOVA at state and national scales. Previous ANOCOVA applications in other regions (Red River Valley, Minnesota for Corwin and Lesch, 2014; and Coachella Valley, California for Corwin and Lesch, 2016) found that different formulations for Eq. (4) performed better (i.e., EC_aH included along with EC_aV), suggesting the ANOCOVA model parameterization is region specific. Future research should focus on determining the factors that define an ANOCOVA region.

Regarding the accuracy of salinity predictions, the remote sensing approach performs worse than the ANOCOVA approach. The performance of the remote sensing model is limited by the quality and type of the covariates (Scudiero et al., 2015). The accuracy of the remote sensing approach can be increased if additional statistically significant covariates (e.g., soil texture, elevation, meteorological data, and crop type) are added to the model (Scudiero et al., 2015). Indeed, when data on soil texture (from laboratory measurements at the 267 soil sampling locations) is used in the model, the *lofo* cross-validation returns an observed-predicted R^2 = 0.70, with RMSPE = 3.90 dS m^{-1}. It is a future challenge for researchers to provide moderate to high resolution soil type/texture maps at large spatial extents, as the currently available information in the USA (i.e., SSURGO maps) is of insufficient accuracy and resolution for use in a remote sensing approach (Scudiero et al., 2014; Scudiero et al., 2015).

The main weakness of the remote sensing approach is predicting salinity at low levels (Fig. 2.d), whereas the ANOCOVA approach performs remarkably better (Fig. 2.a, 2.b, 2.c). Accurate spatial information at low salinity levels is particularly relevant for many agronomical practices, including crop selection and site-specific

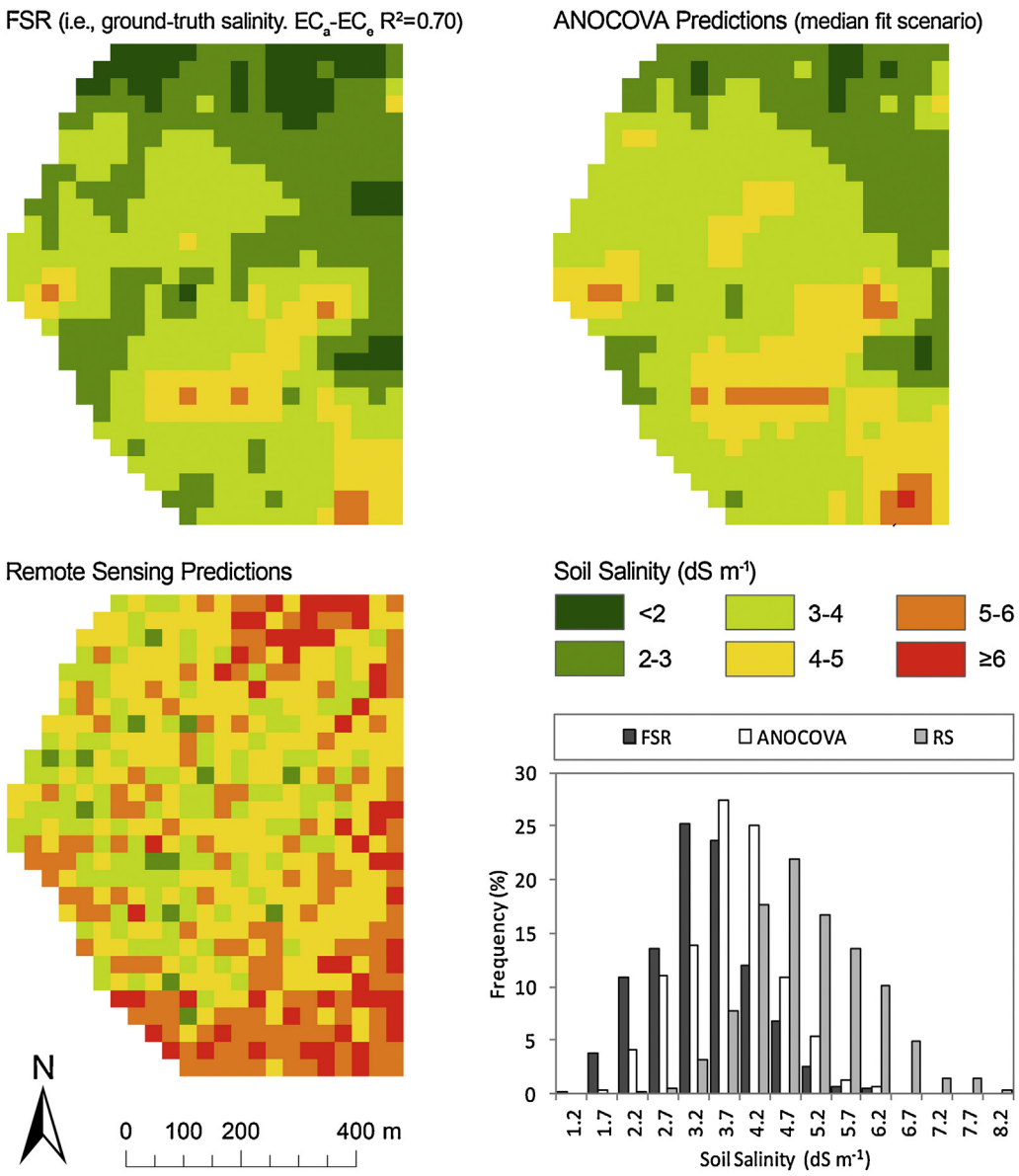

Fig. 3. Soil salinity at Field 13: (a) field specific regression (FSR) estimation of soil salinity using apparent electrical conductivity survey (i.e., ground-truth), (b) analysis of covariance (ANOCOVA) predictions using a single soil sample to estimate the field specific intercept, (c) remote sensing (RS) predictions with model parameterized on the other 21 fields, and (d) histogram showing frequency distribution for soil salinity in the 3 maps.

management (e.g., irrigation). To focus on this inaccuracy issue, let us consider the salinity assessment at Field 13, where the FSR EC_a-EC_e estimations (30×30 m support) are normally distributed and characterized by an average salinity of 3.01 dS m^{-1} and standard deviation of 0.84 (Fig. 3). When the remote sensing model is used to estimate (i.e., *lofo* cross-validation) salinity over such a low range of salinity, high inaccuracy is expected. The remote sensing map is characterized by an average salinity of 4.74, standard deviation of 0.99, and a non-significant ($r = -0.03$) Pearson correlation with the FSR map. This is as expected because when salinity is not a major limiting factor for crop growth, the Landsat 7 surface reflectance spatial variability is driven by other edaphic factors. At low salinity levels, the ANOCOVA approach is more reliable (Fig. 3), with a predicted (i.e., using 1 soil sample to estimate γ_0-median fit *lofo* scenario) average salinity of 3.51 dS m^{-1} and standard deviation of 0.78.

With regards to spatial resolution, the ANOCOVA EC_e map in Fig. 3.b was built at the 30×30 m resolution for the sole aim of matching the Landsat 7 resolution. The resolution of an ANOCOVA (and FSR) map depends solely on the sampling scheme used in the EC_a survey. Hengl (2006) provides some guidelines on how to select the proper pixel size given the available sampling density. Nevertheless, for most site-specific agronomical practices, the 30×30 m resolution is generally adequate.

The ANOCOVA approach outperforms remote sensing modeling in terms of accuracy at low salinity levels, but has clear limitations regarding the spatial scale to which it can be applied. When dealing with a single field, one can use EC_a measurements and soil sampling to estimate EC_e with field-specific calibrations using linear regression modeling or other techniques such as regression kriging. For a larger area, such as an entire farm or a small basin (e.g., 1 km^2), one should employ the ANOCOVA approach. Firstly, a representative (e.g., soil, tillage, irrigation types) number of fields should be used to calibrate the ANOCOVA slope coefficient. Secondly, salinity at the remaining fields can be mapped by means of an EC_a survey and one soil sample per field, used to derive the ANOCOVA field-

specific slope coefficient. When dealing with spatial scales greater than ~1000 ha, surveying fields for EC_a becomes impractical due to both monetary and time constrains. At such spatial scales, remote sensing modeling is the only viable solution. The calibration of a remote sensing model should be suitable for very large areas (i.e., >10 km^2), allowing mapping salinity at much lower costs than with the ANOCOVA approach. These scales of application correspond to those recommended by Corwin and Lesch (2016) where FSR (Eq. (3)) is best for areas less than 1 km^2, ANOCOVA (Eq. (4)) for 1–10 km^2, and remote sensing modeling (Eq. (5)) for 10–10^5 km^2. The remote sensing salinity estimation model by Scudiero et al. (2015) should be applicable to the entire WSJV, but might not be suitable to map salinity in the eastern side of the valley, which has significantly different types of soils. Future research is needed to test the range of applicability of the remote sensing approach with a single parameterization. Can the same parameterization be used for a national or world-wide salinity assessment model, or should its use be limited to a specific region?

6. Conclusions

The ANOCOVA approach to mapping soil salinity is accurate and robust, but time consuming and expensive when applied over tens of thousands of hectares, i.e., regional scale. Compared to the ANOCOVA approach, the remote sensing approach is a less expensive option, particularly at scales above 10 km^2. Unfortunately, the remote sensing approach has lower accuracy when salinity is <10 dS m^{-1} (Scudiero et al., 2015; Wu et al., 2014; Yahiaoui et al., 2015). Consistent with the literature on remote sensing of soil salinity (Allbed et al., 2014; Metternicht and Zinck, 2003; Taghizadeh-Mehrjardi et al., 2014; Wu et al., 2014), Eq. (8) performs well in identifying saline soils. However, the major weakness of the remote sensing approach is higher error at low salinity values when compared to the ANOCOVA approach. Regardless of the unprecedented levels of accuracy obtained by Scudiero et al. (2015), salinity assessment with the remote sensing approach is best used for the categorization of salinity into classes of non-saline (EC_e = 0–2 dS m^{-1}), slightly saline (EC_e = 2–4 dS m^{-1}), moderately saline (EC_e = 4–8 dS m^{-1}), strongly saline (EC_e = 8–16 dS m^{-1}), and extremely saline (EC_e > 16 dS m^{-1}) and should not be used in agricultural decision making (e.g., crop selection, sub-field site-specific irrigation management).

When mapping salinity at spatial scales much greater than the field scale, there is clearly an appropriate scale for each of the two approaches, dictated by resource demands and accuracy requirements. The remote sensing approach is an appropriate tool for classifying large clusters of high and low salinity, which can be very useful for policy makers and water allocation management. The ANOCOVA approach is appropriate to map salinity with fairly high accuracy, at the large farm level, allowing for better decision making and agronomic management.

The two approaches could be used to complement one another. As shown in this manuscript, the two models can be calibrated on the same dataset. Once calibrated, the remote sensing model could be used to map salinity at large spatial extents (i.e., > 10 km^2), whereas the ANOCOVA approach could be used to increase the accuracy of root-zone soil salinity estimations over fields of particular interest (i.e., 1–10 km^2).

Acknowledgements

Partial funding for this research was from the Office of Naval Research (FMMI number: 3200001344). The authors wish to acknowledge the numerous hours of diligent technical work that were performed in the field and in the laboratory by several technicians whose efforts and conscientiousness were crucial to obtaining the data presented, including Wes Clary, Kevin Yemoto, and Michael Bagtang. The authors specifically acknowledge the dedication and technical professionalism of Wes Clary who was crucial in locating field sites in the San Joaquin Valley, conducting EC_a surveys, and analyzing soil samples and Kevin Yemoto who provided technical expertise with GIS and laboratory analyses.

References

Allbed, A., Kumar, L., Sinha, P., 2014. Mapping and modelling spatial variation in soil salinity in the Al Hassa Oasis based on remote sensing indicators and regression techniques. Remote Sens. 6, 1137–1157.
Archie, G.E., 1942. The electrical resistivity log as an aid in determining some reservoir characteristics. Trans. AIME 5, 54–62.
Boryan, C., Yang, Z., Mueller, R., Craig, M., 2011. Monitoring U.S. agriculture: the U.S. Department of Agriculture, National Agricultural Statistics Service, Cropland Data Layer Program. Geocarto Int. 26, 341–358.
Brenning, A., 2012. Spatial cross-validation and bootstrap for the assessment of prediction rules in remote sensing: the R package sperrorest. In: 2012 IEEE International Geoscience and Remote Sensing Symposium (IGARSS), 23–27 July 2012, pp. 5372–5375.
Chang, A.C., Silva, D.B. (Eds.), 2014. Springer, Dordrecht, The Netherlands.
Cliff, A.D., Ord, J.K., 1981. Spatial Processes: Models & Applications. Pion, London, UK.
Cone, T., 1997. The vanishing valley. San Jose Mercury News Magazine, June 29. San Jose Mercury News, pp. 9–15.
Corwin, D.L., Lesch, S.M., 2005a. Apparent soil electrical conductivity measurements in agriculture. Comput. Electron. Agric. 46, 11–43.
Corwin, D.L., Lesch, S.M., 2005b. Characterizing soil spatial variability with apparent soil electrical conductivity: I. Survey protocols. Comput. Electron. Agric. 46, 103–133.
Corwin, D.L., Lesch, S.M., 2013. Protocols and guidelines for field-scale measurement of soil salinity distribution with EC_a-directed soil sampling. J. Environ. Eng. Geophys. 18, 1–25.
Corwin, D.L., Lesch, S.M., 2014. A simplified regional-scale electromagnetic induction—salinity calibration model using ANOCOVA modeling techniques. Geoderma 230–231, 288–295.
Corwin, D.L., Lesch, S.M., 2016. Validation of the ANOCOVA model for regional-scale EC_a-EC_e calibration. Soil Use Manage., http://dx.doi.org/10.1111/sum.12262.
Daly, C., Halbleib, M., Smith, J.I., Gibson, W.P., Doggett, M.K., Taylor, G.H., Curtis, J., Pasteris, P.P., 2008. Physiographically sensitive mapping of climatological temperature and precipitation across the conterminous United States. Int. J. Climatol. 28, 2031–2064.
Ghassemi, F., Jakeman, A.J., Nix, H.A., 1995. Salinisation of Land and Water Resources: Human Causes, Extent, Management and Case Studies. CAB international, Wallingford, Oxon, UK.
Han, W., Yang, Z., Di, L., Mueller, R., 2012. CropScape: a web service based application for exploring and disseminating US conterminous geospatial cropland data products for decision support. Comput. Electron. Agric. 84, 111–123.
Harradine, F.F., 1950. Soils of Western Fresno County California. University of California, Berkeley, California, USA.
Harvey, O.R., Morgan, C.L., 2009. Predicting regional-scale soil variability using a single calibrated apparent soil electrical conductivity model. Soil Sci. Soc. Am. J. 73, 164–169.
Hengl, T., 2006. Finding the right pixel size. Comput. Geosci. 32, 1283–1298.
Huete, A., Didan, K., Miura, T., Rodriguez, E.P., Gao, X., Ferreira, L.G., 2002. Overview of the radiometric and biophysical performance of the MODIS vegetation indices. Remote Sens. Environ. 83, 195–213.
Ivits, E., Cherlet, M., Tóth, T., Lewińska, K., Tóth, G., 2011. Characterisation of productivity limitation of salt-affected lands in different climatic regions of Europe using remote sensing derived productivity indicators. Land Degrad. Dev. 24, 438–452.
Lal, R., Iivari, T., Kimble, J.M., 2004. Soil Degradation in the United States: Extent, Severity, and Trends. CRC Press, Boca Raton, FL, USA.
Lasdon, L.S., Waren, A.D., Jain, A., Ratner, M., 1978. Design and testing of a generalized reduced gradient code for nonlinear programming. ACM Trans. Math. Softw. (TOMS) 4, 34–50.
Lesch, S.M., 2005. Sensor-directed response surface sampling designs for characterizing spatial variation in soil properties. Comput. Electron. Agric. 46, 153–179.
Lesch, S.M., Corwin, D.L., 2008. Prediction of spatial soil property information from ancillary sensor data using ordinary linear regression model derivations, residual assumptions and model validation tests. Geoderma 148, 130–140.
Lesch, S.M., Rhoades, J.D., Corwin, D.L., 2000. ESAP-95 version 2.01 R. User manual and tutorial guide. In: Research Rpt. 146. U.S. Salinity Laboratory, Riverside, CA.
Letey, J., 2000. Soil salinity poses challenges for sustainable agriculture and wildlife. Calif. Agric. 54, 43–48.
Lobell, D.B., Lesch, S.M., Corwin, D.L., Ulmer, M.G., Anderson, K.A., Potts, D.J., Doolittle, J.A., Matos, M.R., Baltes, M.J., 2010. Regional-scale assessment of soil salinity in the Red River Valley using multi-year MODIS EVI and NDVI. J. Environ. Qual. 39, 35–41.

Lobell, D.B., 2010. Remote sensing of soil degradation: introduction. J. Environ. Qual. 39, 1–4.
Masek, J.G., Vermote, E.F., Saleous, N.E., Wolfe, R., Hall, F.G., Huemmrich, K.F., Gao, F., Kutler, J., Lim, T., 2006. A landsat surface reflectance dataset for north america, 1990–2000. IEEE Geosci. Remote Sens. 3, 68–72.
Metternicht, G., Zinck, J., 2003. Remote sensing of soil salinity: potentials and constraints. Remote Sens. Environ. 85, 1–20.
Mulla, D.J., 2013. Twenty five years of remote sensing in precision agriculture: key advances and remaining knowledge gaps. Biosyst. Eng. 11, 358–371.
Rhoades, J.D., Raats, P.A.C., Prather, R.J., 1976. Effects of liquid-phase electrical conductivity water content, and surface conductivity on bulk soil electrical conductivity. Soil Sci. Soc. Am. J. 40, 651–655.
Rhoades, J.D., 1996. Salinity: electrical conductivity and total dissolved solids. In: Sparks, D.L. (Ed.), Methods of Soil Analysis: Part 3—Chemical Methods, SSSA Book Series No. 5. Soil Sci. Soc. Am., Madison, WI, USA, pp. 417–435.
Rouse, J., Haas, R., Schell, J., Deering, D., 1973. Monitoring vegetation systems in the Great Plains with ERTS. Third ERTS Symposium. NASA SP-351 1, 309–317.
Roy, D.P., Ju, J., Kline, K., Scaramuzza, P.L., Kovalskyy, V., Hansen, M., Loveland, T.R., Vermote, E., Zhang, C., 2010. Web-enabled landsat data (WELD): landsat ETM composited mosaics of the conterminous United States. Remote Sens. Environ. 114, 35–49.
Ruß, G., Brenning, A., 2010. Data mining in precision agriculture: management of spatial information. Computational Intelligence for Knowledge-based Systems Design, Lecture Notes in Computer Sciences, 6178. Springer, Heidelberg, Germany, pp. 350–359.
Schoups, G., Hopmans, J.W., Young, C.A., Vrugt, J.A., Wallender, W.W., Tanji, K.K., Panday, S., 2005. Sustainability of irrigated agriculture in the San Joaquin Valley: California. Proc. Natl. Acad. Sci. U. S. A. 102, 15352–15356.
Scudiero, E., Skaggs, T.H., Corwin, D.L., 2014. Regional scale soil salinity evaluation using Landsat 7, Western San Joaquin Valley, California, USA. Geoderma Reg. 2-3, 82–90.
Scudiero, E., Corwin, D.L., Skaggs, T.H., 2015. Regional-Scale soil salinity assessment using Landsat ETM+ canopy reflectance. Remote Sens. Environ. 169, 335–343.
Singh, A., 2015. Soil salinization and waterlogging: a threat to environment and agricultural sustainability. Ecol. Ind. 57, 128–130.
Taghizadeh-Mehrjardi, R., Minasny, B., Sarmadian, F., Malone, B., 2014. Digital mapping of soil salinity in Ardakan region central Iran. Geoderma 213, 15–28.
Tanji, K.K., Wallender, W.W., 2012. Nature and extent of agricultural salinity and sodicity. In: Wallender, W.W., Tanji, K.K. (Eds.), Agricultural Salinity Assessment and Management. ASCE Manuals and Reports on Engineerring Practices No. 71. ASCE, Reston, VA, USA, pp. 10–25.
Tian, Y., Huffman, G.J., Adler, R.F., Tang, L., Sapiano, M., Maggioni, V., Wu, H., 2013. Modeling errors in daily precipitation measurements: additive or multiplicative? Geophys. Res. Lett. 40, 2060–2065.
U.S. Salinity Laboratory Staff, 1954. USDA Handbook No. 60. Diagnosis and Improvement of Saline and Alkali Soils. U.S. Governament Prnting Office, Washington, D.C.
Wu, W., Al-Shafie, W., Mhaimeed, A., Ziadat, F., Nangia, V., Payne, W., 2014. Soil salinity mapping by multiscale remote sensing in Mesopotamia, Irag. IEEE J. Sel. Top. Appl. 7, 4442–4452.
Yahiaoui, I., Douaoui, A., Zhang, Q., Ziane, A., 2015. Soil salinity prediction in the Lower Cheliff plain (Algeria) based on remote sensing and topographic feature analysis. J. Arid Land 7, 794–805.
Zhang, T., Qi, J., Gao, Y., Ouyang, Z., Zeng, S., Zhao, B., 2015. Detecting soil salinity with MODIS time series VI data. Ecol. Ind. 52, 480–489.